

Extraction of Cilium Beat Parameters by the Combined Application of Photoelectric Measurements and Computer Simulation

Larisa Gheber and Zvi Priel

Department of Chemistry, Ben-Gurion University of the Negev, Beer-Sheva 84105, Israel

ABSTRACT Photoelectric signals were created and used to investigate the features of the signals as a function of the ciliary beat parameters. Moreover, correlation between the simulated and the measured signals permitted measurement of the cilium beat parameters. The simulations of the signals were based on generation of a series of time-frozen top-view frames of an active ciliary area and determination of the amount of light passing through an observation area in each of these frames. All the factors that might contribute to the shape of the signals, namely, partial ciliary transmittance of light, three-dimensional ciliary beat (composed of recovery, effective, and pause parts), phase distribution on the ciliary surface, and the large number of cilia that contribute to the photoelectric signal, were taken into account in generation of the signals. Changes in the ciliary parameters influenced the shape of the photoelectric signals, and the different phases of the beat could not be directly and unequivocally identified in the signals. The degree of temporal asymmetry of the beat and the portion of the cycle occupied by the pause significantly influenced the shapes of both the lower and the upper parts of the signal and the slopes of the signal. Increases in the angle of the arc swept by the cilium during the effective stroke smoothed the signals and increased the duration of the upper part of the signal. The angle of the arc projected by the cilium onto the cell surface during the recovery stroke had minor effects on the signal's shape. Characteristics of the metachronal wave also influenced the signal's shape markedly. Decreases in ciliary spacing smoothed the signals, whereas ciliary length had a minor influence on the simulated photoelectric signals. Comparison of the simulated and the measured signals showed that the beat parameters of the best-fitting simulated signals converged to values that agree well with the accepted range of beat parameters in mucociliary systems.

INTRODUCTION

Mucociliary systems consist of cilia, which undergo a nearly periodic beating, and an overlying layer of secreted mucus with which the cilia interact to transport loads over the epithelial surface (Spungin and Silberberg, 1984). To propel mucus, each cilium beats in a periodic and asymmetric manner. The ciliary beat consists of a fast effective stroke in the plane perpendicular to the cell surface and a slow recovery stroke in a clockwise direction (top view), during which the cilium returns to its initial position, moving in a plane inclined to the cell surface. Occasionally there is a pause after the effective stroke. The propulsion of mucus takes place during the fast effective stroke when the ciliary tips penetrate the mucus layer and push the mucus in the direction of the effective stroke (Sleigh, 1982; Sleigh et al., 1988). Although this general picture is now accepted, very little is known about the characteristics of the ciliary beat under different experimental conditions.

On an active ciliary area there is usually a phase difference between beating cilia, which creates a wave. This phenomenon is called the metachronal wave, or metachronism (Machemer, 1974; Sleigh, 1974). The metachronal wave in each system has distinct characteristics such as frequency, wavelength, and wave direction, and the last-

named is usually different from the effective stroke direction (ESD). Knight-Jones (1954) defined the main types of metachronism in terms of the angles formed between the direction of the metachronal wave and the ESD. When the wave propagates parallel or antiparallel to the ESD, the metachronism is defined as synplectic or antiplectic, respectively; the type of metachronism is defined as laeoplectic or dexioplectic if the effective stroke is performed to the left or to the right, respectively, of the wave propagation. The properties of the metachronal wave define the number of cilia per unit area that are simultaneously involved in the transport process (Gheber and Priel, 1994). Recently it was shown that the direction of the wave propagation depends strongly on the type of metachronism in the direction of the effective stroke and on the polarization in time and in space of the ciliary beat. Moreover, the metachronal wavelength is found to depend on the following parameters: ciliary length, angle of the arc projected onto the cell surface by the ciliary tip during the recovery stroke, degree of asymmetry of ciliary beat, and portion of the cycle occupied by the pause (Gheber and Priel, 1990b).

Over the years, attempts have been made to measure the parameters of ciliary beating in mucus-propelling cilia (Aiello and Sleigh, 1977; Sanderson and Sleigh, 1981; Marino and Aiello, 1982; Weaver and Hard, 1985; Rautiainen et al., 1992, 1993). Most of these studies were performed with a light microscope supplemented by fast cinematography that photographed ciliary motion at a rate of a few hundred pictures per second. This technique required reconstruction of the three-dimensional motion from a two-dimensional

Received for publication 7 May 1996 and in final form 7 October 1996.

Address reprint requests to Dr. Zvi Priel, Department of Chemistry, Ben-Gurion University of the Negev, Beer-Sheva, 84105, Israel. Tel.: 972-7-6461184; Fax: 972-7-6900046; E-mail: alon@bgumail.bgu.ac.il.

© 1997 by the Biophysical Society

0006-3495/97/01/449/14 \$2.00

pictures. The high magnifications required of the photography because mucus-propelling cilia are short (5–7 μm) and quite dense (100–400 cilia per cell) resulted in incomplete focusing of the cilia during the whole beat cycle. Despite this hindrance, fast cinematography has yielded a general description of the ciliary beat cycle in mucus-propelling cilia from frog oropharyngeal (Aiello and Sleight, 1977), cultured rabbit tracheal (Sanderson and Sleight, 1981), and human respiratory cells (Marino and Aiello, 1982; Rautainen et al., 1992, 1993). In newt lungs, well-defined parameters of the ciliary beat were quantitatively assessed (Weaver and Hard, 1985). However, the time-consuming frame-by-frame analysis dictated that only a small number of cycles be analyzed (Weaver and Hard, 1985).

The activity of mucus-propelling cilia fluctuates greatly on a time scale that ranges from seconds to minutes (Aiello et al., 1991; Eshel et al., 1985; Gheber and Priel, 1990a; Kennedy and Ranyard, 1983; Puchelle et al., 1982; Romet et al., 1991; Weiss et al., 1992). Even when the frequency is constant in time, strong fluctuations in phase can occur (Eshel and Priel, 1987; Ovadyahu and Priel, 1989; Gheber and Priel, 1990a; Ben-Shimol et al., 1991). It has also been found that the beat parameters of the giant frontal cirri of *Stylonychia* undergo fluctuations as a function of time (Mogami et al., 1992). It is reasonable to assume, therefore, that the parameters of the beat of mucus-propelling cilia also exhibit a high degree of fluctuation. For this reason it is necessary to average over very large ensembles and to record over relatively long periods of time. Fast cinematography, which is a tedious and expensive technique, is too limited to be used routinely for measurements of the beating parameters in mucus-propelling cilia.

An alternative approach to this problem, which we employed in the current study, is the use of photoelectric techniques to measure ciliary beat parameters. With these techniques the ciliary beat frequency is routinely obtained (Aiello et al., 1991; Dalhamn and Rylander, 1962; Eshel et al., 1985; Hard and Cypher, 1992; Johnson et al., 1991; Lee and Verdugo, 1976; Ovadyahu et al., 1988; Puchelle et al., 1982; Weiss et al., 1992; Wong et al., 1991; Zahm et al., 1986). Frequency, however, is not the only parameter expressed in the photoelectric signal. Recently it was shown that the shape of the photoelectric signal can be used as a measurable parameter to describe ciliary harmony (Ingels et al., 1992). Inasmuch as the photoelectric signals are a result of the superposition of beating cilia, it is tempting to assume that with an appropriate approach the ciliary beat parameters could also be extracted from the signals. Given the relative ease with which photoelectric measurements can be carried out, it should be relatively easy, therefore, to assess ciliary beat parameters. Until now, however, there has been little attempt to understand the influence of the different aspects of ciliary motility on the photoelectric signals.

Pioneering research in this field was done by Sanderson and Dirksen in 1985. They estimated the temporal parameters of the beat from the shapes of the photoelectric signals obtained from cultured rabbit epithelium and mytilus gill.

However, the possible contribution of the spatial parameters of the beat and the metachronal wave characteristics to the signals obtained were neglected (Sanderson and Dirksen, 1985). In a theoretical study, Rabinovitch and Rabinovitch (1989) investigated the form of the signals as a function of ciliary motion. But, because of the large number of parameters, the movement of cilia was assumed to be two dimensional in the plane of the effective stroke only, and the phase shifts between cilia were introduced only in this direction, reflecting a symplectic metachronal wave.

We propose to expand on this idea, using photoelectric signals to measure the temporal and the spatial parameters of ciliary beating for areas in which a pronounced phase shift with distance is observed. The photoelectric signals are created by the beating of the cilia and therefore are a superposition of the ciliary activity in the observed area. In fact, the characteristics of the beating cilia (frequency, phase shifts, wavelength and direction of the metachronal wave, and form of the beat of a single cilium) and their length and arrangement are all reflected in the shape of the resultant photoelectric signals. The extent to which these different characteristics influence the signals is unknown. Moreover, it is a priori not evident that it is possible to deconvolute the measured signals, i.e., to the ciliary characteristics.

We simulated photoelectric signals and used them to depict the effect of changes of each of the parameters on the features of the photoelectric signals. We found that the shape of the simulated signals is strongly influenced by some ciliary beat and metachronal wave parameters. However, none of the ciliary beat parameters can be unequivocally related to the particular characteristics of the signal, but determination of the ciliary beat parameters based on the shape of photoelectric signals was possible by comparison of the measured and the simulated signals.

EXPERIMENTAL PROCEDURES

The experiments were carried out on a monolayer tissue culture of frog esophagus (*Rana ridibunda*) by a procedure described previously (Eshel et al., 1985). Ciliary activity was monitored by simultaneous measurement of the scattered light from three small active ciliary areas (Gheber and Priel, 1994). A tissue culture, which was transparent to light, was viewed with an inverted microscope (Olympus, IMT, Japan) illuminated by a 100-W tungsten-halogen lamp. The scattered light was collected by three optical fibers (50 μm in diameter), two in the focal plane of the oculars and one in the focal plane of the camera port. An objective magnification of 20 \times was usually used, corresponding to an observation area 2.5 μm in diameter. Objective magnifications of 10 \times and 40 \times , which varied according to the dimensions of area examined, were also used. The photoelectric signals obtained were further amplified by independent systems and sampled continuously for 20–40 s.

Simulation of the photoelectric signals

The photoelectric signals were obtained by collection of the light either passing through or reflected by an examined ciliated area. Here we deal only with the transmission case. We generated computer-simulated photoelectric signals by calculating the amount of light transmitted through a simulated ciliary epithelium as a function of time. The simulations of photoelectric signals are based on creating a series of time-frozen pictures of a top view of the ciliary surface. In each time-frozen picture (frame) the amount of light transmitted through a given observation area was calculated. The time-dependent transmitted light array represents the simulated photoelectric signal because it describes the change in the intensity of light as a function of time. In the following section we describe the simulations and emphasize the parameters involved.

Geometric parameters of the ciliary surface

Ciliary length (L) and spacing between adjacent cilia (D) are geometric parameters that are constant for a given ciliary area. Their values in mucociliary systems, 5–7 μm for L and 0.5–0.8 μm for D , are well established (Sleigh, 1990; Sleigh et al., 1988). Ciliary bases were assigned to be equally spaced on the cell surface, with rows parallel and columns perpendicular to the direction of the effective stroke.

Beat of a single cilium

The first step in the creation of the simulated signal is simulation of the mode of movement of a single cilium. The beat was simulated according to the accepted beat form, consisting of a fast effective stroke in which the cilium is nearly straight, a pause, and a slow recovery stroke during which the cilium returns to the initial position with a bend propagating from the ciliary base to the tip. Side and top views of the accepted form of the ciliary beat are shown in Fig. 1 A. The form of a typical computer-simulated ciliary cycle is shown in Fig. 1 B.

The duration of the ciliary beat cycle (τ) is determined by the ciliary beat frequency F : $\tau = 1/F$. The durations of the effective, pause, and recovery phases of the beat are assigned as τ_e , τ_p , and τ_r , respectively. The degree of temporal asymmetry of the beat (Rt) is defined as the ratio of the duration of the recovery stroke to the duration of the effective stroke. Therefore, Eqs. 1 and 2 summarize the connections between the temporal parameters of the beat:

$$\tau_e = (1/F - \tau_p)/(1 + Rt), \quad (1)$$

$$\tau_r = \tau_e Rt. \quad (2)$$

Inasmuch as the ciliary beat frequency F is measured by all the photoelectric techniques, then, based on Eqs. 1 and 2, the number of free parameters that one needs to characterize the temporal parameters of the ciliary beat fully is two.

In the computer simulations a cilium performing an effective stroke is represented by a straight line (Fig. 1 B). The initial angle of the effective stroke, measured between the cilium at the beginning of the effective stroke and the cell surface, is θ_i . The angle swept by the cilium during the effective stroke is θ_e , and the final angle of the effective stroke is θ_f (Fig. 1 B ii). For simplicity, we assume that the initial and the final angles of the effective stroke are identical ($\theta_i = \theta_f$). This is a reasonable assumption based on the descriptions of the ciliary beat in frog palate (Aiello and Sleigh, 1972) and rabbit tracheal epithelium (Sanderson and Sleigh, 1981). Therefore the initial and the final angles of the effective stroke can easily be calculated if θ_e , the angle swept by the cilium during the effective stroke, is known, according to Eq. 3:

$$\theta_i = \theta_f = (180 - \theta_e)/2. \quad (3)$$

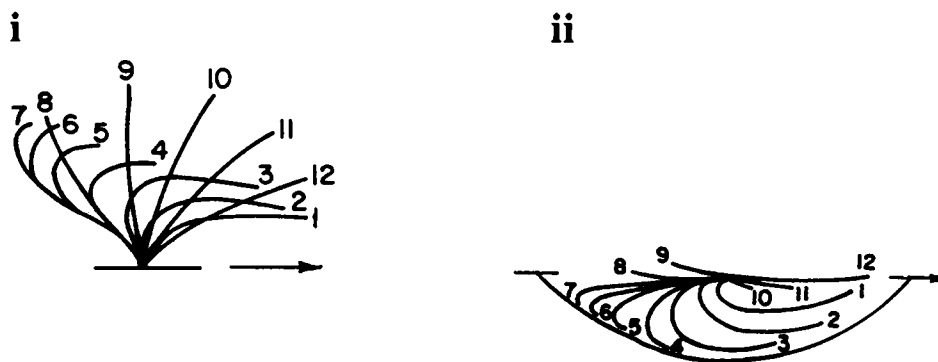
During the recovery stroke the ciliary tip projects a curved line on the cell surface, which is nearly an arc of a circle (Fig. 1 A ii). In the simulations we approximated this line by an arc of angle θ_r (Fig. 1 B iii). The angle of this arc represents the deviation of the cilium that is performing the recovery stroke from the plane of the effective stroke and, therefore, can be regarded as the amplitude of the recovery stroke. The angle θ_r had not been measured previously, but it can easily be estimated from descriptions of the top views of the beat cycles of mucus-propelling cilia that were presented in a number of studies (Aiello and Sleigh, 1972; Marino and Aiello, 1982; Sanderson and Sleigh, 1981). From these reports it is evident that this angle is close to 60° and that it is smaller than θ_e . The ratio between the angle swept by the cilium during the effective stroke, θ_e , and the angle swept by the ciliary tip on the cell surface during the recovery stroke, θ_r , measures the degree of spatial asymmetry of the ciliary beat (Ra), as shown in Eq. 4:

$$Ra = \theta_e/\theta_r. \quad (4)$$

The larger the angle θ_e , the more pronounced the amplitude of the effective stroke and the higher the spatial asymmetry of the beat. On the other hand, the larger the angle θ_r , relative to θ_e , the more conical the beating and the lower the spatial asymmetry of the beat.

During the recovery stroke a bend, which propagates from ciliary base to tip, is usually observed (Fig. 1 A). To simulate the projection of this bend on the cell surface we constructed a ciliary projection during this stroke from two lines. The contact point of these two lines represents the projection of the ciliary bend on the cell surface (Fig. 1 B iii). During the simulation of the recovery strokes this contact point moved along the arc of the circle at an angle $\theta_r + 10^\circ$. The string of the bend arc was four-fifths of the string of the tip arc. The strings of the two arcs (the arc of the bend and the arc of the tip) were collinear. The two arcs had one mutual point at the beginning of the effective stroke (Fig. 1 B iii). During the simulations more than 10 different combinations of strings and angles of the bend arc were

A



B

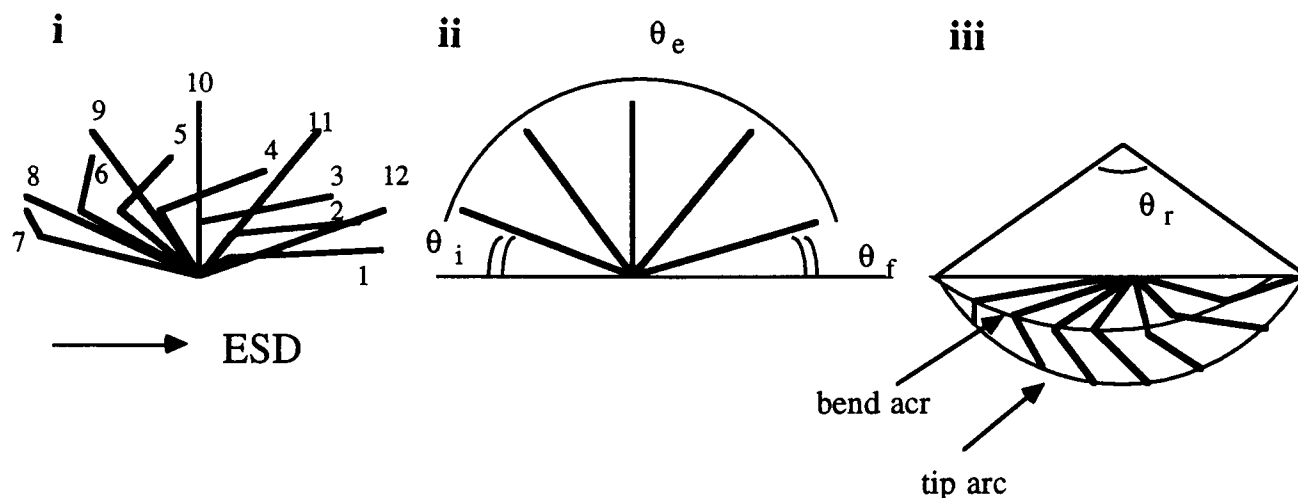


FIGURE 1 Form of a single ciliary beat. **A**, General form of the beat based on reports of various mucociliary systems (Sleigh, 1974; Aiello and Sleigh, 1977; Sanderson and Sleigh, 1981). Twelve different stages during the beat cycle are shown in the top (*i*) and side (*ii*) views. Stages 1–7, recovery stroke; stages 8–12, effective stroke. The pause phase is between stages 12 and 1. The ESD is indicated by the arrow. The recovery stroke is performed clockwise. **B**, Typical beat cycle (stages 1–12) created by the simulation program. A side view of the whole cycle (*i*), a side view of the effective stroke (*ii*), and a top view of the recovery stroke (*iii*) are shown. θ_e , angles of the arc swept by the cilium during the effective stroke; θ_i , θ_f , initial and final angles, respectively, of the effective stroke; θ_r , angle of arc projected onto the cell surface by the ciliary tip during the recovery stroke (*tip arc*); *bend arc*, arc of the projection of the ciliary bend created during the recovery stroke on the cell surface. The ESD is indicated by an arrow. The recovery stroke is performed clockwise.

examined. No significant differences were detected among results obtained with different bend arcs and strings.

Top view of an active ciliary area

To simulate an active ciliary area the only additional information required is the values of the delay times between cilia in two directions. This information permits the determination of the stages of all the cilia in the array relative to the first one. The times of delay between cilia parallel (Δt_x) and perpendicular (Δt_y) to the ESD can now be measured simultaneously (Gheber and Priel, 1994).

After the stage of the first cilium in the array was assigned, the stages of all the other cilia in the row parallel to the ESD were assigned based on the measured time of delay in this direction, Δt_x (Fig. 2 *A*). Then the stage of the first cilium in the second row was determined according to the time of delay between cilia perpendicular to the ESD (Δt_y). The stages of the cilia in the second row were then determined according to Δt_x , as was done for the first row (Fig. 2 *B*). This procedure was continued for all the rows until a full time-frozen picture (frame) of a ciliary array was created.

After the stages of all the cilia in the array were determined, their projections on the cell surface were calculated.

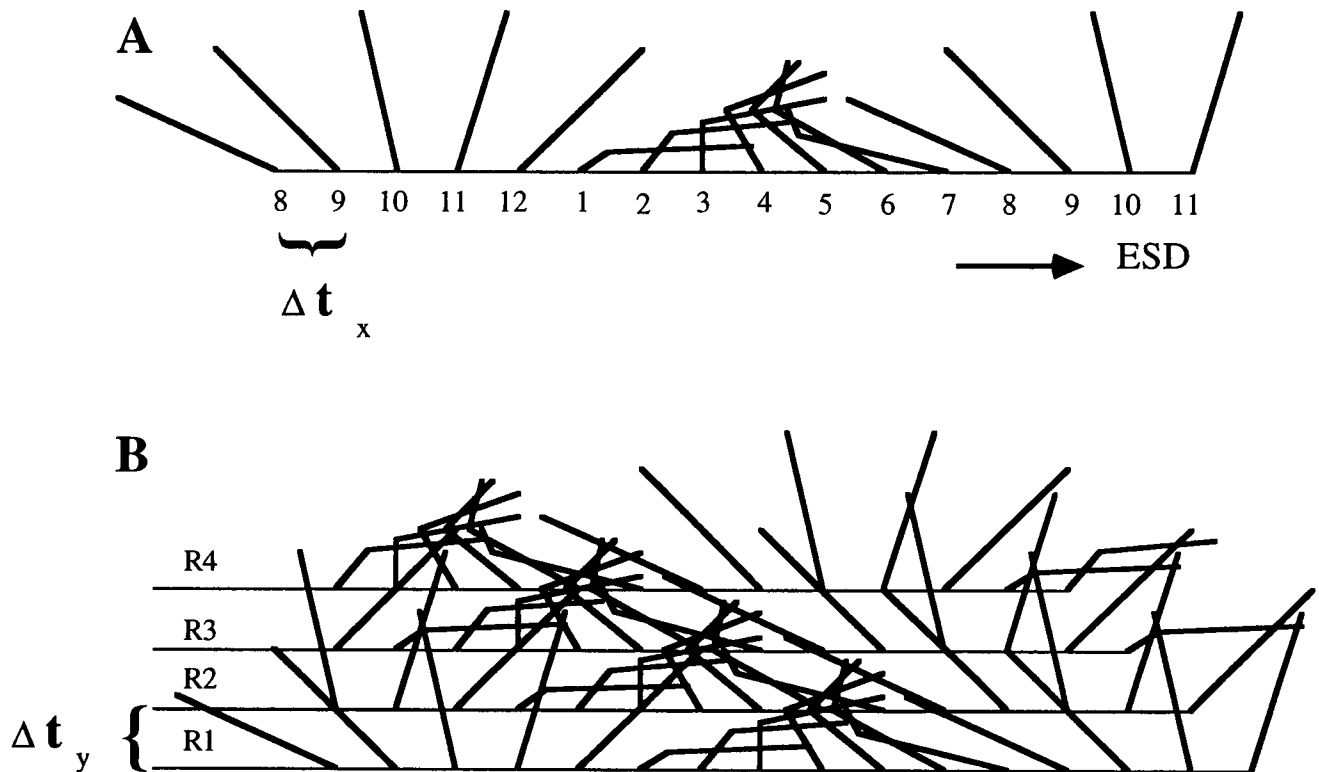


FIGURE 2 Schematic representation of a time-frizzed picture of active ciliary epithelium involved in metachronal coordination. Cilia go through 12 different stages during the cycle. Stages 1–7 represent the recovery stroke, and stages 8–12 represent the effective stroke, as in Fig. 1 *B*. Times of delay between adjacent cilia parallel (Δt_x) and perpendicular (Δt_y) to the ESD are indicated and can be determined by simultaneous three-point measurements (Gheber and Priel, 1994). *A*, After the stage of the first cilium in the row parallel to the ESD (indicated by an arrow) was assigned at the beginning of the effective stroke, the stages of all the cilia in this row were determined according to the time of delay between cilia parallel to the ESD, Δt_x . *B*, The stages of the cilia in the adjacent rows (R2–R4) were determined according to the first row (R1) and the time of delay between cilia perpendicular to the ESD, Δt_y . In this example $\Delta t_y = 2\Delta t_x$.

The projections during the effective stroke and the pause were calculated by simple trigonometry from knowledge of the ciliary length and the angle at which the cilium is inclined above the surface. During the recovery stroke the positions of three points on the cell surface, namely, the positions of the base, the ciliary tip, and the bend projections, are known for each cilium. As the recovery stroke propagates, the positions of the tip and bend projections change (Fig. 1 *B iii*), defining the projection of the cilium on the cell surface in different stages of the recovery stroke.

The observation area of most of the devices used, including ours (Eshel et al., 1985; Gheber et al., 1995), is round. Therefore we analyzed the data from a round observation area. The area of the simulated ciliary array, however, is considerably larger than the observation area of the optical device. Because the cilia are quite long (6 μm) compared with typical radii of the observation area (in our setup 1.25, 2.5, or 5 μm , corresponding to objective magnifications of 40 \times , 20 \times , and 10 \times , respectively) and the ciliary beat form is three dimensional and highly asymmetric in space, a large number of cilia whose bases are not in the area of observation enter this observation area during different stages of their motion. It is impossible to measure only the cilia whose bases are within the observation area. Even if the

area of observation is as small as a ciliary cross-section, more than one cilium will interfere with the light passing through the area of observation.

To account for all the cilia that contribute to the photoelectric signal, we took the size of the ciliary array in simulations as a rectangle whose length was parallel to the ESD. During the effective stroke the most distant cilia to enter the observation area are those whose projections reach the observation area at the end of the effective stroke (from one side of the observation area) or at the beginning of the effective stroke (from the other side). Therefore, the length of the rectangle was taken as the sum of the ciliary projections at the beginning and the end of the effective stroke and the diameter of the observation area. Following similar considerations, but during the recovery stroke, the width was taken as the sum of the ciliary length and the diameter of the observation area. Because of the asymmetric form of ciliary beat, the number of cilia that interfere with light in the observation area varies as a function of time and is difficult to determine analytically. The dimensions of the rectangle were assigned to take into account the maximal number of cilia that may contribute to the photoelectric signal in any time during the cycle. For the ciliary parameters described above, a spacing between adjacent cilia of

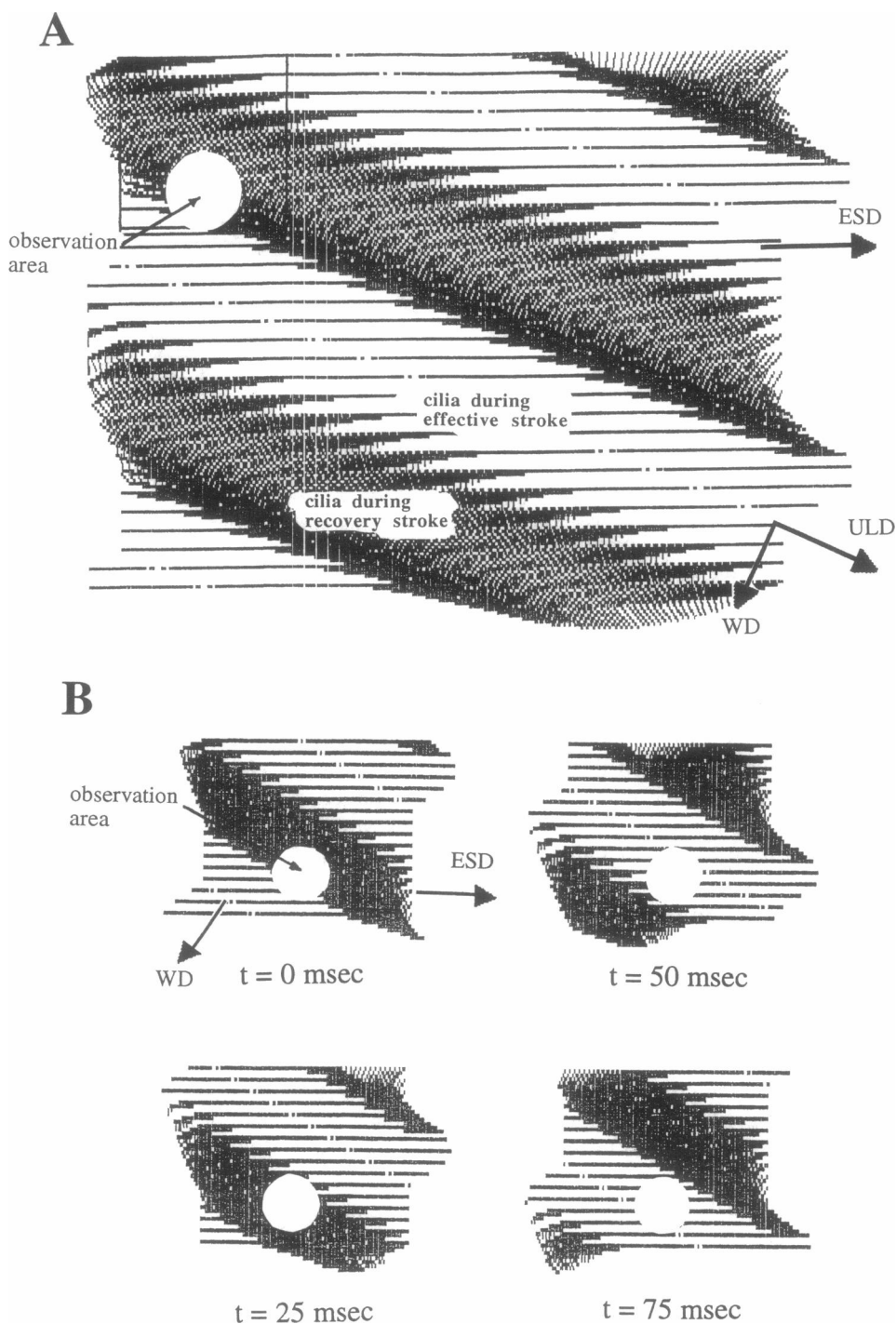
0.5 μm , and an observation area diameter of 2.5 μm , the rectangle contained 250 cilia, whereas ~ 150 cilia contribute instantaneously to the simulated signal. Inasmuch as in each frame only the cilia that actually contributed were taken into account, we introduced no artifact by simulating the movement of larger number of cilia. The resulting top-view pictures, which include cilia in effective, pause, and recovery phases, are shown in Fig. 3 A.

Generation of the simulated photoelectric signal

The optical response of cilia consists of absorption, reflection, and refraction. It was recently shown (Rabinovich and Rabinovich, 1989) that the main contribution of a single cilium to light flux through a unit area is of the form

$$I_t = I_0 \exp(-\beta u), \quad (5)$$

FIGURE 3 Top view of a time-frozen ciliary area involved in metachronal coordination as obtained by the simulation program. The phase shifts between cilia in two directions were measured by the three-simultaneous-points technique; the ciliary motion was simulated as described in the text. Cilia in different stages and metachronal wave fronts (uniphase lines) are clearly seen. The ESDs and the directions of wave propagation are indicated by arrows. The observation area in each case is indicated by a white circle. The pictures are not to scale. **A**, Simulation of a large ciliary area. The direction of uniphase lines (ULD) is indicated. **B**, Simulation of four small ciliary areas as a function of time (indicated beneath each frame). The beat period in this example is 100 ms. It is clearly seen that different amounts of light are measured by the photodetector as a function of time.



where I_t and I_0 are the transmitted and the initial light intensities, respectively, u is the effective ciliary width, and β is a coefficient that expresses ciliary interference with transmitted light. Because cilia are densely packed and their beating is asymmetric, it is possible that a number of cilia, which are at different heights above the cell surface, will shade over the same segment. In such a case the transmittance (T) through the segment will be given by

$$T = I_t/I_0 = \exp(-\gamma i), \quad (6)$$

where γ is a coefficient that includes the effective ciliary width ($\gamma = \beta u$) and i is the number of cilia above the segment. The value of γ may vary as a function of tissue type, ciliary characteristics, and source of light. Therefore its estimation is quite difficult. We have examined the shapes of simulated signals in several cases of γ (see below).

To simulate changing light intensity as a function of time, we calculated the amount of light transmitted through the observation area in every frame. The area of observation was divided into small segments ($0.04 \mu\text{m}^2$), and the light-intensity transmission through each segment was calculated according to Eq. 6. The light intensity was then integrated over the entire observation area. After the transmitted light intensity in the first frame was calculated, the next frame was created. The state of the first cilium in the array was changed, and the stages and projections of all the other cilia in the array were determined according to the delay times in two directions (Fig. 2). This procedure was repeated until the first cilium completed one beat cycle and returned to its initial position at the beginning of the effective stroke. The time interval between the frames was determined by the sampling rate. In our laboratory a sampling rate of 360 Hz is commonly used, which corresponds to 2.78-ms intervals between frames. The result, after completion of one beat cycle, was a time-dependent array that represented the photoelectric signal, in which the light intensity alternated as a function of time (Fig. 3 B).

Analysis of the signals

To investigate the influence of ciliary parameters on the shape of the simulated signal, we defined several characteristics of the simulated signal that were examined as a function of beat parameters. The duration ratio (D_r) is defined by

$$D_r = a/b, \quad (7)$$

where a is the duration of the part of the signal that is above its average level and b is the duration of the part that is below its average level (Fig. 4). We also measured the slopes of the signals. We have assigned S_1 as the slope of the increasing part of the signal (from minimum to maximum) and S_2 as the slope of the decreasing part of the signal (from maximum to minimum); see Fig. 4. The slopes were

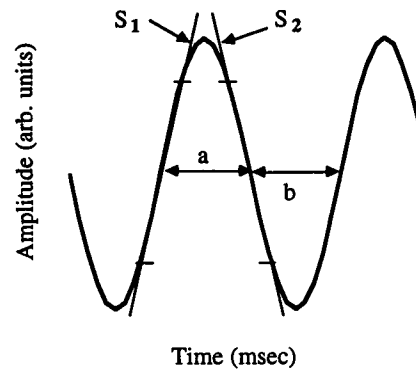


FIGURE 4 Parameters for analysis of the simulated signals. D_r is the ratio of durations of the upper part of the signal to the lower part; $D_r = a/b$. S_1 is the slope of the increasing part of the signal (from minimum to maximum); S_2 is the slope of the decreasing part of the signal (from maximum to minimum)

measured at 50% of peak-to-peak signal amplitude, near the middle of the signal.

Correlation between the measured and the simulated signals

We estimated the beat parameter by finding a set of beating parameters that created simulated signals that showed good correlation with the measured photoelectric signals. After the simulated signals were created, the fit was calculated in two ways: least squares and Pearson correlation analysis. The two methods led to the same results. The time interval for the fit calculation was one cycle (90–100 ms). We corrected the possible phase difference between the measured and the simulated signals by shifting the measured cycle in time until the best correlation was obtained.

RESULTS AND DISCUSSION

Simulated active ciliary area

The simulation program generates time-frozen, top-view pictures of an active ciliary epithelium (Fig. 3). In these pictures, areas of varying degrees of lightness, corresponding to cilia in different stages of the cycle, can be seen clearly. During the effective stroke, when cilia are nearly perpendicular to the cell surface, the size of projection on the cell surface is relatively small. On the other hand, during the recovery stroke the projections created by the cilia on the cell surface are larger because of their closeness to the cell surface and the fact that cilia move closer to one another. This effect can be seen clearly in Fig. 2, in which cilia during the effective stroke are spread whereas cilia during the recovery stroke are close to one another. This leads to the conclusion that during the effective stroke the shadow produced by the cilia is smaller than that produced during the recovery because cilia moving closer together during the recovery stroke are expected to interfere more effectively with light. Therefore, in Fig. 3 the darker parts of

the ciliary array represent cilia in the recovery phase and the lighter parts represent cilia in the effective phase.

Because during the recovery stroke the cilia move close together (Fig. 2) and create dark areas on the cell surface (Fig. 3), the lower parts of the signals obtained, which correspond to smaller amounts of light, are created when the majority of the cilia in the observation area are in different stages of the recovery stroke. By the same token, the upper part of the signal is created when most of the cilia in the observation area are in the effective phase. Inasmuch as the lower part of the signal is created primarily by the recovery stroke, the larger the portion of the cycle occupied by the recovery stroke, the larger is the lower part of the signal (relative to the upper part).

The dark and the light areas are arranged in lines (Figs. 2 and 3), which are uniphase or synchrony lines. These lines are a manifestation of the metachronal wave. The consecutive times of delay between cilia often occur in two directions on an active ciliary surface (Machemer, 1974). In mucociliary systems the apparent coordination parallel to the ESD is antiplectic (Sleigh et al., 1988). The apparent wave perpendicular to the effective stroke is symplectic because the wave component in this direction is created during and by the recovery stroke (Gheber and Priel, 1990b; Sleigh, 1982). As a result, the metachronal wave direction is backward and to the right of the ESD (Fig. 3). With time propagation, the uniphase lines move in the direction of the metachronal wave propagation, causing different degrees of dark, or shadow, to be seen in the observation area (Fig. 3 B). This change in light intensity as a function of time, which is always observed when cilia are studied under the microscope, create the pseudoperiodic signals obtained by all photoelectric methods.

Form of the simulated photoelectric signals

To evaluate whether the simulated signals could be used to measure the ciliary beat parameters, we first investigated the influence of the ciliary parameters on the shapes of the signals. Because a large number of parameters were involved it was important to determine which were the dominant ones and what their influence was.

Typical normalized photoelectric signals created by simulation are shown in Figs. 5–9. In each signal one cycle was duplicated to emphasize the signal shape. We have assumed that during one beat cycle all the parameters of the ciliary beat were constant. As the duration of the measured cycles was relatively short, 30–120 ms (corresponding to a ciliary beat frequency of 8–30 Hz), this assumption was quite reasonable, in spite of the fluctuating nature of mucociliary activity (Eshel and Priel, 1986; Gheber and Priel, 1990a, 1994; Kennedy and Duckett, 1981). Indeed, it has been shown by Monte Carlo calculations that an average period of fluctuation in frequency is greater than 100 ms (Eshel et al., 1985).

Partial transmittance of light by a single cilium

One of the factors that determine the basic type of photoelectric signal obtained is γ (Eq. 6). The value of γ reflects the degree to which a single cilium prevents the transmittance of light through a segment of area. Fig. 5 demonstrates the effect of increasing γ on the signal shape. The signal shapes are quite complicated, with some containing an additional, local maximum (Fig. 5 A). The amplitude of this additional maximum decreases with decreasing transmittance of a single cilium (increasing γ). For γ values less than 0.7 (50% transmittance) it appears in the lower part of the signal and can be considered a local minimum (Fig. 5 A). An increase in the portion of the cycle occupied by the pause smooths the signals and diminishes the additional peak (compare Fig. 5 A and B).

The shapes of the signals created with relatively high or low γ do not vary as a function of ciliary beat parameters (not shown). When $\gamma > 1$, the signal shape is quite smooth, and the double-peaked signals reported by Sanderson and Dirksen (1985) are not obtained. On the other hand, for $\gamma < 0.5$, most of the signals have a double-maxima shape, and the typically smooth signals measured in our lab (Eshel et al., 1985) and by others (Aiello et al., 1991) are seldom obtained. In the γ range 0.7–1, signals are sensitive to

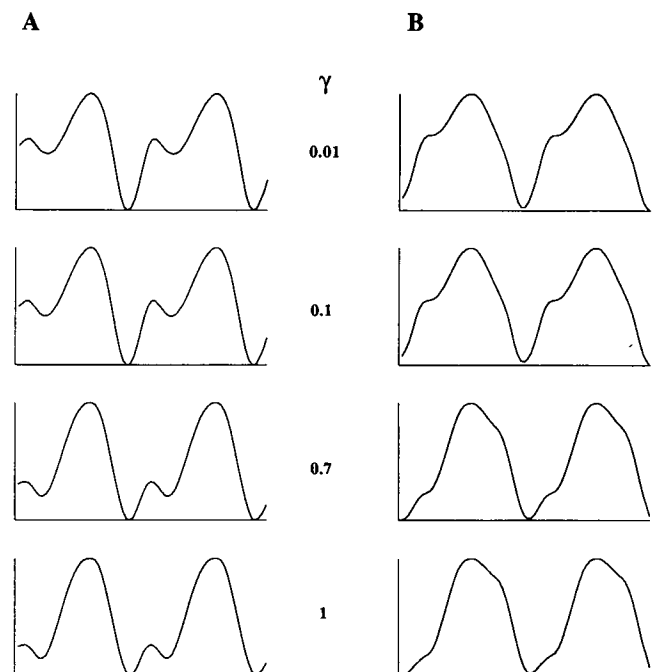


FIGURE 5 Influence of the degree of ciliary transmittance on the shape of the simulated signal. One cycle of the simulated signal was duplicated and normalized. Each pair of signals (*left and right*) was created with the same value of γ (Eq. 6), indicated between the two signals. In the left panel (A) the duration of pause $\tau_p = 0\%$ of the cycle. In the right panel (B) $\tau_p = 20\%$. The other parameters were $L = 6 \mu\text{m}$, $D = 0.5 \mu\text{m}$, $F = 10 \text{ Hz}$, $Rt = 3$, $\theta_r = 60^\circ$, $Ra = 2.5$, $\Delta t_x = 2.7 \text{ ms}$, $\Delta t_y = 5.4 \text{ ms}$, and observation area diameter $2.5 \mu\text{m}$. The corresponding transmittance values of a single cilium (T) are the following (see Eq. 6): for $\gamma = 0.01$, $T = 99\%$; for $\gamma = 0.1$, $T = 90\%$; for $\gamma = 0.7$, $T = 50\%$; and for $\gamma = 1$, $T = 37\%$.

change in ciliary beat parameters, and smooth as well as double-shaped signals can be obtained (Figs. 7–9). Therefore, it can be concluded that for mucociliary systems the value of γ is in the range $0.7 \geq \gamma \geq 1$. We investigated the influence of ciliary parameters on the signal shape created with $\gamma = 0.7$ (Figs. 7–9 and Table 1) and $\gamma = 1$ (not shown). The signals created with these two values of γ showed a similar dependence of signal shape on the ciliary parameters, with minor differences in the absolute values of the slopes (S_1 , S_2) and duration ratios (D_r).

Size of the observation area

Within a given cross-sectional area of the photodetector the objective magnification in use determined the size of the observation area and the shape of the photoelectric signal obtained (Fig. 6). With increasing area of observation (decreasing magnification), a smoother signal, with a more moderate transition between maxima and minima, was obtained (Fig. 6). The change in the shape of the signal shown in Fig. 6 was obtained with all other ciliary parameters remaining constant. Changes in ciliary beating parameters influenced the shape of photoelectric signals (see Fig. 8). However, the extent of this influence decreased as the area of observation increased, although the general features remained similar (not shown). This result indicates that one must use small areas of observation to study the form of the

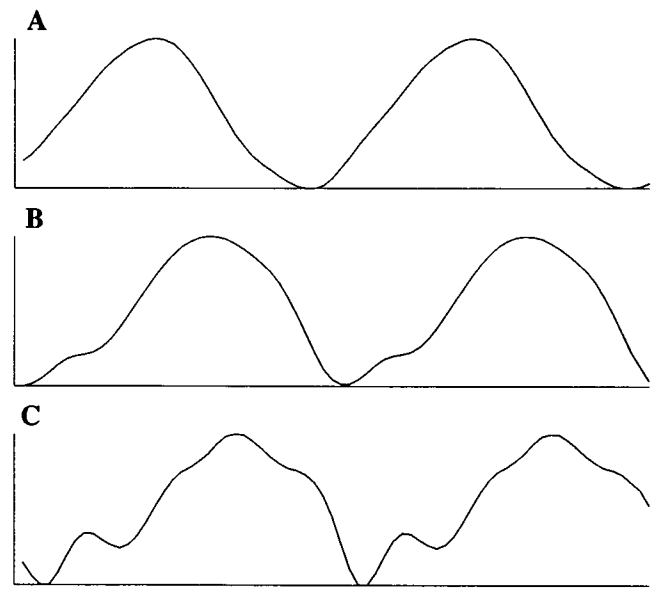


FIGURE 6 Influence of the area of observation on the shape of simulated signals. One cycle of simulated signal was duplicated and normalized. The observation area diameters were A, 5 μm ; B, 2.5 μm ; and C, 1.25 μm . $\gamma = 0.7$. All the other ciliary parameters were constant and were identical to those for Fig. 5.

ciliary beat from the photoelectric signals. However, signals obtained from an area of 1.25- μm diameter (in our experimental system equivalent to 40 \times magnification; Eshel and Priel, 1986), although they exhibit good sensitivity of signal shape to the ciliary parameters, present experimental problems in the determination of the beating parameters because of the restricted amount of light that can pass through such a small observation area and the decrease in the signal-to-noise ratio (Ben-Shimol et al., 1991). An observation area 2.5 μm in diameter (in our system, magnification of 20 \times) also gives good sensitivity of signal shape to beat parameters (Fig. 6). This magnification gives smooth signals with satisfactory signal-to-noise ratios (Eshel and Priel, 1986). For these reasons, both measurements and simulations studied in our lab were usually performed at 20 \times objective magnification with an observation area diameter of 2.5 μm (Gheber and Priel, 1990a, 1994; Weiss et al., 1992; Gheber et al., 1995; Tarasiuk et al., 1995).

Ciliary length and spacing

For a given ciliary area, geometric parameters such as ciliary spacing and length are constant. However, small variations in the values of these parameters are observed, even within the same mucociliary system (Puchelle et al., 1984). We found that a change in ciliary length in the 5–9- μm range did not significantly affect the signal shape (Fig. 7A). Increasing the spacing between cilia from 0.5 to 0.9 μm caused a secondary peak to appear before the major maximum (Fig. 7B) but did not significantly change the duration ratio of the cycle and signal slopes (not shown).

TABLE 1 Influence of the metachronal wave parameters on the shape of the photoelectric signals

Δt_x (ms)	Δt_y (ms)	λ (μm)	α (deg)	D_r	S_1	S_2
5.4	5.4	6.5	135	1.25	14.5	21.3
5.0	5.0	7.1	135	1.40	14.2	22.8
4.5	4.5	7.8	135	1.25	13.5	22.4
4.0	4.0	8.8	135	1.25	13.7	22.1
3.5	3.5	10.1	135	1.10	15.3	23.2
3.0	3.0	11.8	135	1.00	17.8	25.5
2.7	2.7	13.1	135	1.00	20.3	26.7
2.7	5.4	8.3	115	0.89	16.9	26.1
3.0	5.4	8.1	119	0.89	15.3	25.9
3.5	5.4	7.8	123	1.00	14.1	25.3
4.0	5.4	7.4	126	1.25	13.7	23.4
4.5	5.4	7.1	130	1.25	13.7	22.2
5.4	5.4	6.5	135	1.25	14.5	21.3
5.4	5.4	6.5	135	1.25	14.5	21.3
5.4	4.5	7.1	140	1.25	15.6	21.3
5.4	4.0	7.4	143	1.40	15.9	21.3
5.4	3.5	7.8	147	1.40	15.6	20.9
5.4	3.0	8.1	151	1.40	15.7	20.8
5.4	2.7	8.3	153	1.40	15.7	20.7

The duration ratio (D_r) and the slopes (S_1 and S_2) of the simulated signals were calculated as a function of various times of delay between adjacent cilia in directions parallel (Δt_x) and perpendicular (Δt_y) to the direction of the effective stroke changed. The metachronal wavelength (λ) was $\lambda = (D \sin(\arctan(\Delta t_x/\Delta t_y)))/(\Delta t_x F)$. The angle between the direction of the wave propagation and the effective stroke (α) was $\alpha = 90^\circ + \arctan(\Delta t_x/\Delta t_y)$ (see, for an explanation, Gheber and Priel (1990, 1994)). The constant parameters were $F = 10$ Hz, $\tau_p = 0\%$, $Rt = 2$; $Ra = 2$, $\theta_r = 60^\circ$, and observation area diameter 2.5 μm .

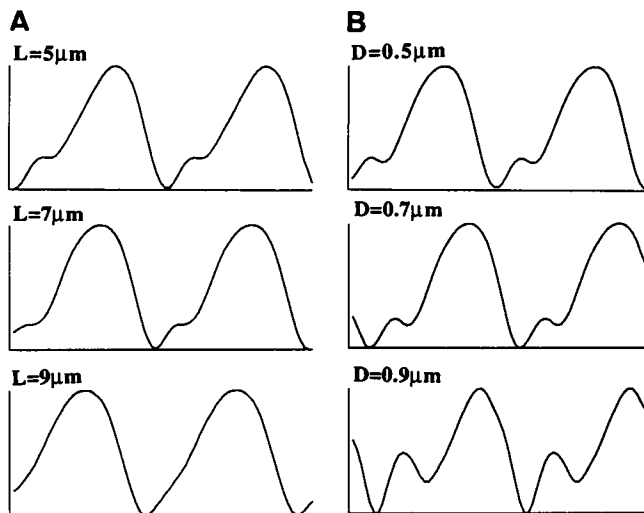


FIGURE 7 Influence of ciliary length (A) and ciliary spacing (B) on signal shape. A, The ciliary length (L) is indicated in the upper left corner of each panel. B, Spacing between cilia (D) is indicated in the upper left corner of each panel. All other ciliary parameters were constant and identical to those in Fig. 5, $\gamma = 0.7$.

When the ciliary spacing increases, the moving cilia are more spread out, and the amount of transmitted light changes. During the recovery stroke, less-dense areas appear, and the shape of the signal in this part becomes more complex.

Metachronal coordination

We recently found that the metachronal wavelength in cultured frog esophagus epithelium varies in the 5–9- μm range and that the wave component parallel to the ESD is more than twice as long as the component perpendicular to the ESD (Gheber and Priel, 1994). This implies that the time of delay parallel to the ESD should also be shorter. Therefore, we checked the influence of change in the times of delay and the consequent change in the metachronal wave parameters on the shape of the photoelectric signals (Table 1). The values for the times of delay were chosen within the range that corresponds to the metachronal wave characteristics in mucociliary systems (Sleigh et al., 1988).

We found that, as the metachronal wavelength increases from 6.5 μm to 13 μm , the slopes of the signals increase (Table 1). The slopes of the signals reflect the number of frames during the beat cycle that produce intermediate degrees of shading on the cell surface. These frames probably include stages at the beginning or at the end of both the effective and the recovery strokes. Increases in the slopes reflect a faster change from light to dark owing to the decrease in the number of these frames. Indeed, one obtains a faster transition between the lower and the upper parts of the signals by decreasing the times of delay between the adjacent cilia in both directions (Table 1). Assuming that the times of delay are equal in both directions, decreasing them

causes an increase in the metachronal wavelength, a decrease in duration ratio (Dr), and an increase in the slopes of the signals. Cilia will beat synchronously if $\Delta t_x = \Delta t_y = 0$. Therefore, relatively small values of the times of delay in both directions cause almost synchronous ciliary beating, which will lead to sharper transitions from light to dark, i.e., an increase in signal slopes. A change in the direction of the wave propagation from laeoplectic to antyplectic coordination caused an increase in the duration ratio (Dr) of the signal. These results clearly indicate that both metachronal wavelength and wave direction influence the form of the photoelectric signals obtained, and therefore the contribution of the metachronal wave properties to the signal shape should be taken into account when one is deriving information, other than frequency, from these signals.

Beat parameters

To investigate the influence of the ciliary beating parameters on the photoelectric signals, we generated series of signals, varying a single parameter in each series while keeping the other parameters constant (Fig. 8). The varied parameters were Rt , τ_p , Ra , and θ_r (see their definitions in the preceding section; also note that $Ra \times \theta_r = \theta_e$). The parameter ranges were chosen according to the values expected for these parameters in mucociliary systems (Aiello and Sleigh, 1977; Sanderson and Sleigh, 1981; Marino and Aiello, 1982; Sanderson and Dirksen, 1985).

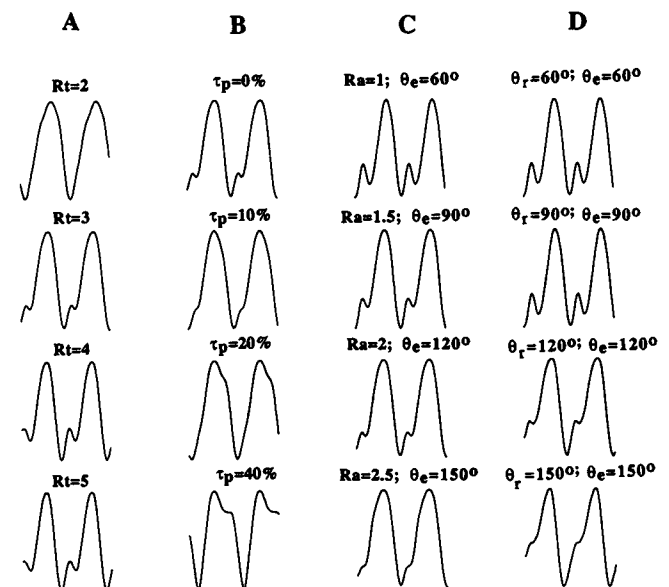


FIGURE 8 Series of simulated signals generated with various ciliary beat parameters. In each column (A–D) one ciliary beat parameter was varied, while the other parameters remained constant. The values of the varying parameters are indicated on top of each signal. Because the angle of the effective stroke (θ_e) changes as a function of Ra , θ_r , or both, its value was also indicated when Ra or θ_r was changed. The values of the constant parameters are $F = 10$ Hz, $L = 6$ μm , $D = 0.5$ μm , $Rt = 2$, $\tau_p = 0\%$, $\theta_r = 60^\circ$, $Ra = 2$, $\Delta t_x = 2.7$ ms, $\Delta t_y = 5.4$ ms, observation area diameter 2.5 μm , and $\gamma = 0.7$.

The temporal parameters of the beat, Rt and τ_p , markedly influence the simulated signals because they change the signals' general form, duration ratio, and slopes (Fig. 8 A and B and Table 2). Inasmuch as the lower part of the cycle is related to the recovery stroke, changes in duration of this stroke are expected to influence the duration ratio (D_r) directly. An increase in temporal asymmetry of the beat (increase in Rt) or a decrease in the pause duration (decrease in τ_p) results in a direct increase in proportion of the cycle occupied by the recovery stroke. Indeed, these two effects increase the lower part of the signal (Fig. 8 A and B), which is reflected in the decrease of D_r as a result of an increase in Rt , a decrease in τ_p , or both (Table 1).

As the proportion of the cycle occupied by the recovery stroke (increasing Rt) was increased, an additional peak (local maximum) was observed in the lower part of the signal, before the major peak (Fig. 8 A). The appearance of this secondary peak was due to the increase in the signal slopes observed with increasing Rt (Table 1). This secondary peak should be related to the enlarged number of ciliary states that appear during the recovery stroke. However, in spite of the obvious connection between the secondary peak and the recovery stroke, not all the stages of the recovery strokes were expressed in the secondary peak. When $Rt = 2$, $F = 10$ Hz, and $\tau_p = 0\%$ (the first signal in Fig. 8 A), the duration of the recovery stroke is 67 ms. However, in this signal the secondary peak was not observed (Fig. 8 A). Therefore, the area of the secondary peak cannot be used directly to measure the duration of this stroke.

As the pause duration was increased, the secondary peak related to the recovery stroke disappeared, and a new bend

gradually appeared on the right-hand side of the signal maximum (Fig. 8 B). When the pause duration was increased markedly this bend turned into a plateau that represented frames with constant shading in which most of the cilia were in the pause position (last signal in Fig. 8 B). The disappearance of the secondary peak on the left of the maximum and the appearance of the plateau on the right of the maximum caused an increase of the signal slope S_1 in the pause duration range of $30\% > \tau_p > 50\%$ and caused a decrease of the slope S_2 in the pause duration range of $0\% > \tau_p > 10\%$ (Table 2).

The plateau created by the increase in pause appeared in the upper part of the signal, indicating that the shading produced by the cilia during the pause was less than the shading produced during the recovery stroke. This can be explained by the close packing of cilia during the recovery stroke (Fig. 2) and by the fact that, because of the phase difference, large numbers of cilia could be at different heights during the recovery stroke, shading over the same point. This contradicts the interpretation of the signal shape performed by Sanderson and Dirksen (1985). However, in their report, phase differences between cilia were neglected. We also observed the appearance of similar plateaus with increasing τ_p for γ values of 0.1 and 1 (not shown). Therefore, it is quite clear that, during the pause, there is more shading than during the effective stroke and less shading than during the recovery stroke.

With respect to the geometric parameters of the ciliary beat, the angle of an arc swept by the cilium during the effective stroke caused the most pronounced effects on the signal shape. An increase in this angle significantly smoothed the signals (Fig. 8 C) and broadened their upper part, which was reflected in the increasing duration ratio of the signal (D_r) (Table 2). One can obtain an increase in θ_e by either increasing Ra with constant θ_r (Fig. 8 C) or increasing θ_r with constant Ra (Fig. 8 D). The changes in the simulated signal shapes in these two cases were very similar (compare Fig. 8 C and D). There was an apparent decrease in the slope S_1 induced by increasing θ_r (Table 2). However, this decrease in slope actually resulted from smoothing of the secondary peak owing to increasing θ_e (Fig. 8 C and D), an effect that occasionally occurs near the middle of the signal (Fig. 8 D, bottom panel), in the region where the slopes are calculated (see Fig. 4). Therefore the decrease in S_1 reflected not a significant θ_r influence on the signal shape but rather a significant influence of θ_e on the signal shape. The effects of θ_r were sufficiently minor that they can be regarded as a constant. The value of this angle is near 60° , as judged from reconstructed fast cinematography pictures reported by a number of investigators (Aiello and Sleight, 1977; Sanderson and Sleight, 1981; Marino and Aiello, 1982).

In summary, we have found that the properties of the metachronal wave and the ciliary beating parameters significantly influence the signal shape. As the metachronal wavelength increases, the slopes of the signal also increase, indicating fast transition between lower and upper parts of

TABLE 2 Influence of the ciliary parameters on the parameters of the photoelectric signals: duration ratio (D_r) and signal slopes (S_1 , S_2)

Parameters Varied		D_r	S_1	S_2
$Rt = 1$		1.40	14.4	24.0
$= 2$		0.89	17.0	26.1
$= 3$		0.71	17.9	27.3
$= 4$		0.63	17.0	28.0
$= 5$		0.63	17.7	28.8
$\tau_p = 0\%$		0.89	16.9	26.0
$= 10\%$		1.11	16.9	22.0
$= 20\%$		1.40	15.9	22.7
$= 30\%$		1.80	17.5	22.0
$= 40\%$		2.30	21.8	21.5
$= 50\%$		2.00	26.7	22.0
$Ra = 1.0$	$\theta_e = 60^\circ$	0.63	18.0	26.9
$= 1.5$	$= 90^\circ$	0.71	17.1	27.0
$= 2.0$	$= 120^\circ$	0.89	17.0	26.1
$= 2.5$	$= 150^\circ$	1.11	18.0	24.0
$\theta_r = 60^\circ$	$\theta_e = 60^\circ$	0.63	17.9	26.0
$= 90^\circ$	$= 90^\circ$	0.80	14.0	28.3
$= 120^\circ$	$= 120^\circ$	0.80	14.0	27.1
$= 150^\circ$	$= 150^\circ$	0.80	10.0	28.2

The constant parameters are $F = 10$ Hz, $L = 6$ μm , $D = 0.5$ μm , $\tau_p = 0\%$, $Rt = 2$, $Ra = 2$, $\theta_r = 60^\circ$, $\theta_e = 120^\circ$, $\Delta t_x = 2.7$ ms, $\Delta t_y = 5.4$ ms, observation area diameter 2.5 μm , $\gamma = 0.7$.

the signal. Changing the angle of wave propagation from 115° to 163° relative to the ESD increased mainly the upper part of the signal (increase in D_r). Ciliary parameters, specifically the degree of temporal asymmetry of the beat and the portion of the cycle occupied by the pause, influence both the distribution of the lower and the upper parts of the signal (D_r) and the signal slopes (S_1 , S_2). The angle of the effective stroke was also found to influence the shape of the signal dramatically, whereas the angle of the recovery stroke had minor effects. A decrease in spacing between adjacent cilia smoothed the simulated signals obtained. The sensitivity of the signal shape to change in the ciliary beat parameters strongly suggests that the ciliary beat parameters can be extracted from the measured photoelectric signals.

Comparison between simulated and sampled signals

Although it is clear that the recovery stroke constitutes the lower part of the signal and the effective stroke the upper part, the different phases of the cycle could not be directly identified in the simulated signals. Similar results were recently reported by others (Ingels et al., 1994). We found in the present study that even when the signals have a multiextrema shape, as was reported in culture tracheal epithelium (Lansley et al., 1992; Sanderson and Dirksen, 1985), the interpretation of the signal shape is quite complicated and the different peaks cannot be directly related to the specific phase of the beat.

Because direct evaluation of the beat parameters from the shape of the signals is practically impossible, we determined the ciliary beating parameters by comparing measured and simulated signals. We generated 3 sets of 45 simulated signals with changing beat parameters, each set with a different value of γ , and correlated them with the measured signals. The principal assumption in this approach was that the set of parameters used to yield the best fit for the simulated signals would be a fitting description of the ciliary parameters at the time of the photoelectric signal sampling.

The values of the beat parameters were chosen such that one of the values would be in the lower limit of the accepted range for this parameter, one in the upper limit, and at least one in the middle of the range. Because θ_r has only a minor influence on the signal shape (Fig. 8 C and D), its value was taken as a constant, 60° . The ciliary beat frequency and the times of delay between cilia in two directions were measured by the three-simultaneous-points technique (Gheber and Priel, 1994). The values for the beat parameters were $Rt = 1, 3, 5$; $\tau_p = 0\%, 20\%, 40\%$; and $Ra = 0.5, 1, 1.5, 2, 2.5$; consequently, $\theta_e = 30^\circ, 60^\circ, 90^\circ, 120^\circ, 150^\circ$.

We checked the fit of 30 cycles, measured under normal conditions. In Fig. 9 the two best-fitting simulated signals to one measured cycle (dashed curves) are presented for three different values of γ . The ciliary beat parameters for the best-fitting cycles are given beneath each panel. Despite the

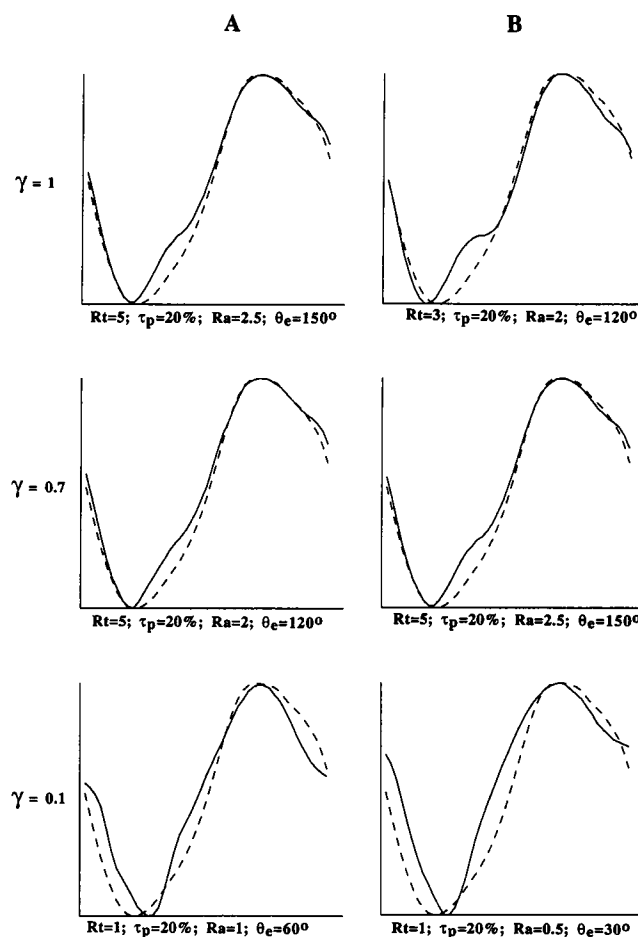


FIGURE 9 Comparison between one measured cycle and one simulated cycle. In each panel, one simulated cycle (solid curve) and one measured cycle (dashed curve) are drawn. For each set, created with different γ values (indicated at the left), the best-fitting cycle is shown in A and the second best in B. The values of the beating parameters used to create the best-fitting simulated cycles are indicated beneath each panel. The values of the constant parameters determined by simultaneous-three-point measurement in our experimental setup were $F = 10.5$ Hz, $\Delta t_x = 2.7$ ms, $\Delta t_y = 5.4$ ms, and observation area diameter $2.5 \mu\text{m}$. Other constant parameters were $L = 6 \mu\text{m}$, $D = 0.5 \mu\text{m}$, and $\theta_r = 60^\circ$.

fact that the intervals between values of the variable parameters were quite large and the number of simulated signals was quite small, the best fits obtained were quite good. By decreasing the intervals between the input parameters (which would increase the number of simulated signals), better correlation could possibly be obtained. In most of the cycles the fit obtained for γ values of 0.7 and 1 was better than the fit obtained for γ values of 0.1.

The beating parameters of the best-fitting simulated signals for $\gamma = 0.7$ or $\gamma = 1$ were consistent with the values shown in Fig. 9, namely, relatively high temporal asymmetry of the beat ($Rt = 3$ or $Rt = 5$), a pause duration larger than 0%, and a relatively large angle of the effective stroke, $90^\circ < \theta_e < 150^\circ$. On the other hand, the parameters of the best-fitting signals created with $\gamma = 0.1$ showed low temporal asymmetry ($Rt = 1$) and small angles of the effective

stroke arc ($\theta_e = 30^\circ, 60^\circ$). For $\gamma = 0.7$, the values of the beat parameters averaged over 30 cycles (mean \pm SE) were correlation, 0.98 ± 0.002 ; $Rt = 3.4 \pm 0.3$; $\tau_p = 15.3\% \pm 1.5\%$; $Ra = 2.1 \pm 0.4$; $\theta_e = 120^\circ \pm 10^\circ$. Similar results were obtained for $\gamma = 1$. For $\gamma = 0.1$ the following parameters were obtained: correlation, 0.95 ± 0.002 ; $Rt = 1.5 \pm 0.2$; $\tau_p = 22\% \pm 1.2\%$; $Ra = 1.0 \pm 0.05$; $\theta_e = 60^\circ \pm 5^\circ$. The better correlation obtained for $\gamma = 0.7$ and $\gamma = 1$ suggest that signals created with these γ values better describe ciliary activity expressed in the measured photoelectric signals.

In mucociliary systems, under normal conditions, it is accepted that the effective stroke is 2–5 times faster than the recovery stroke, the duration of the pause is not zero, and the angle of the effective stroke is greater than 100° (Aiello and Sleight, 1977; Sanderson and Sleight, 1981; Marino and Aiello, 1982). The ciliary beat parameters obtained from the best-fitting signals created with $\gamma = 0.7$ or $\gamma = 1$ are in good agreement with these values. On the other hand, the parameters created with $\gamma = 0.1$ are far from the accepted range for mucociliary systems. These results, in addition to the better correlation obtained between the measured cycles and the cycles created with higher values of γ (Fig. 9), clearly indicate that γ values higher than 0.7 describe the mucociliary systems well and that the comparison between simulated and measured signals can be used to measure the beating parameters in mucociliary systems.

Ciliary beat parameters in mucociliary systems may change as a function of time and as a result of changing experimental conditions. Because of experimental difficulties, there has been very little effort to measure these changes quantitatively. The facts that changes in the beat parameters induce significant changes in the shape of simulated photoelectric signals (Fig. 8) and that the parameters of the best-fitting simulated signals created for $\gamma = 0.7$ or $\gamma = 1$ agree with the values of these parameters reported in literature support the assumption that comparison between simulated and measured photoelectric signals can be used to measure the parameters of the ciliary beat.

CONCLUDING REMARKS

We have demonstrated that the photoelectric signals obtained by measuring the light transmitted through an active ciliary epithelium can be used to determine the parameters of the ciliary beat. This comprehensive investigation of the dependence of the photoelectric signal shape on ciliary parameters revealed that most of the parameters of ciliary beat, geometry, and metachronal coordination influence the signal shape. As a result of this complex interrelationship between the ciliary parameters and the signal shape, the values of the parameters could not be determined directly, and were, therefore, assessed by comparison between measured and simulated signals.

The main problem with the simulation approach is the large number of parameters that are involved. Here we

reduced the number of free parameters to only four because of the availability of the apparatus that we developed (Gheber and Priel, 1994), which makes possible the simultaneous measurement of cilia beat frequency and the times of delay between cilia in two directions. Moreover, the number of free parameters can be reduced even further (to two free parameters only) by use of the mathematical relationships that tie the ciliary parameters to times of delay (Gheber and Priel, 1990b). However, use of the theoretical model will require further work to adjust the general mathematical relationships to the specific system examined. The correspondence between measured and simulated signals is quite high; however, higher accuracy can easily be achieved, if needed, by introduction of smaller intervals in the free parameter values.

Finally, we believe that we have developed an easy and reliable method for measurement of ciliary beat parameters based on large ensembles. Moreover, this method will permit changes in ciliary beat parameters to be followed under changing experimental conditions in real time.

This research was supported by a grant from the Fund for Basic Research, administered by the Israel Academy of Science and Humanities.

REFERENCES

- Aiello, E., J. Kennedy, and C. Hernandez. 1991. Stimulation of frog ciliated cells in culture by acetylcholine and substance P. *Comp. Biochem. Physiol.* 99:497–509.
- Aiello, E., and M. A. Sleight. 1972. The metachronal wave of lateral cilia of *Mytilus edulis*. *J. Cell Biol.* 54:493–506.
- Aiello, E., and M. A. Sleight. 1977. Ciliary function of the frog oropharyngeal epithelium. *Cell Tissue Res.* 178:267–278.
- Ben-Shimol, Y., I. Dinstein, A. Meisels, and Z. Priel. 1991. Ciliary motion features from digitized video photography. *J. Comp. Assist. Microscopy.* 3:103–116.
- Dalhamn, T., and R. Rylander. 1962. Frequency of ciliary beat measured with a photo-sensitive cell. *Nature (London)*. 196:592–593.
- Eshel, D., Y. Grossman, and Z. Priel. 1985. Spectral characterization of ciliary beating: variations of frequency with time. *Am. J. Physiol.* C160–C165.
- Eshel, D., and Z. Priel. 1986. Spectral characterization of ciliary beating. Biological meaning of the spectral linewidth. *Biophys. Chem.* 23: 261–265.
- Eshel, D., and Z. Priel. 1987. Characterization of metachronal wave of beating cilia on frog's palate epithelium in tissue culture. *J. Physiol.* 388:1–8.
- Gheber, L., and Z. Priel. 1990a. Ciliary activity under normal conditions and under viscous load. *Biorheology.* 27:547–557.
- Gheber, L., and Z. Priel. 1990b. On metachronism in ciliary systems: a model describing the dependence of the metachronal wave properties on the intrinsic ciliary parameters. *Cell Motil. Cytoskel.* 16:167–181.
- Gheber, L., and Z. Priel. 1994. Metachronal activity of cultured mucociliary epithelium under normal and stimulated conditions. *Cell Motil. Cytoskel.* 28:333–345.
- Gheber, L., Z. Priel, C. Aflalo, and V. Shoshan-Barmatz. 1995. Extracellular ATP binding proteins as potential receptors in mucociliary epithelium: characterization using [32 P]3'-O-(4-benzoyl)benzoyl ATP, a photoaffinity label. *J. Membr. Biol.* 147:83–93.
- Hard, R., and C. Cypher. 1992. Reactivation of newt lung cilia: evidence for a possible temperature- and MgATP-induced activation mechanism. *Cell Motil. Cytoskel.* 21:187–198.

- Ingels, K. J., M. R. Nijziel, K. Graamans, and E. H. Huizing. 1994. Influence of cocaine and lidocaine on human nasal cilia. Beat frequency and harmony in vitro. *Arch. Otolaryngol. Head Neck Surg.* 120: 197–201.
- Ingels, K. J., H. L. vanStrien, K. Graamans, G. F. Smoorenburg, and E. H. Huizing. 1992. A study of the photoelectrical signal from human nasal cilia under several conditions. *Acta Otolaryngol. Stockholm.* 112: 831–838.
- Johnson, N. T., M. Villalon, F. H. Royce, and P. Verdugo. 1991. Auto-regulation of beat frequency in respiratory ciliated cells. Demonstration by viscous loading. *Am. Rev. Respir. Dis.* 144:1091–1094.
- Kennedy, J. R., and K. E. Duckett. 1981. The study of ciliary frequencies with an optical spectrum analysis system. *Exp. Cell Res.* 135:147–156.
- Kennedy, J. R., and J. R. Ranyard. 1983. Morphology and quantitation of ciliated outgrowths from cultured rabbit tracheal explants. *Eur. J. Cell Biol.* 29:200–208.
- Knight-Jones, E. W. 1954. Relations between metachroism and the direction of ciliary beat in metazoa. *Q. J. Microsc. Sci.* 95:503–521.
- Lansley, A. B., M. J. Sanderson, and E. R. Dirksen. 1992. Control of the beat cycle of respiratory tract cilia by Ca^{2+} and cAMP. *Am. J. Physiol.* 263:L232–L242.
- Lee, W. I., and P. Verdugo. 1976. Laser light-scattering spectroscopy. A new application in the study of ciliary activity. *Biophys. J.* 16: 1115–1119.
- Machemer, H. 1974. Ciliary activity and metachronism in protozoa. In *Cilia and Flagella*, M. A. Sleight, editor. Academic Press, London. 199–286.
- Marino, M. R., and E. Aiello. 1982. Cinemicrographic analysis of beat dynamics of human respiratory cilia. *Cell Motil. Suppl.* 1:35–39.
- Mogami, Y., J. Pernberg, and H. Machemer. 1992. Ciliary beating in three dimensions: steps of a quantitative description. *J. Math. Biol.* 30: 215–249.
- Ovadyahu, D., D. Eshel, and Z. Priel. 1988. Intensification of ciliary motility by extracellular ATP. *Biorheology.* 25:489–501.
- Ovadyahu, D., and Z. Priel. 1989. Characterization of metachronal wave in beating cilia: distribution of phases in space. *Biorheology.* 26:677–685.
- Puchelle, E., A. Petit, and J. J. Adnet. 1984. Fine structure of the frog palate mucociliary epithelium. *J. Microsc. Cytol.* 16:273–282.
- Puchelle, E., J. M. Zahm, and P. Sadoul. 1982. Mucociliary frequency of frog palate epithelium. *Am. J. Physiol.* 242:C31–C35.
- Rabinovitch, A., and R. Rabinovitch. 1989. A simple model of light transmission through metachronally moving cilia. *J. Appl. Phys.* 67: 1108–1112.
- Rautiainen, M., S. Matsune, S. Shima, K. Sakamoto, Y. Hanamure, and M. Ohyama. 1992. Ciliary beat of cultured human respiratory cells studied with differential interference microscope and high speed video system. *Acta Otolaryngol. Stockholm.* 112:845–851.
- Rautiainen, M., S. Matsune, M. Yoshitsugu, and M. Ohyama. 1993. Degeneration of human respiratory cell ciliary beat in monolayer cell cultures. *Eur. Arch. Otorhinolaryngol.* 250:97–100.
- Romet, S., D. Schoevaert, and F. Marano. 1991. Dynamic image analysis applied to the study of ciliary beat on cultured ciliated epithelial cells from rabbit trachea. *Biol. Cell.* 71:183–190.
- Sanderson, M. J., and E. R. Dirksen. 1985. A versatile and quantitative computer-assisted photoelectronic technique used for the analysis of ciliary beat cycles. *Cell Motil.* 5:267–292.
- Sanderson, M. J., and M. A. Sleight. 1981. Ciliary activity of cultured rabbit tracheal epithelium: beat pattern and metachrony. *J. Cell Sci.* 47: 331–347.
- Sleight, M. A. 1974. Metachronism of cilia of metazoa. In *Cilia and Flagella*, M. A. Sleight, editor. Academic Press, London. 287–304.
- Sleight, M. A. 1982. Movement and coordination of tracheal cilia and the relation of these to mucus transduction. *Cell Motil. Suppl.* 1:19–24.
- Sleight, M. A. 1990. Ciliary adaptation for the propulsion of mucus. *Biorheology.* 27:527–532.
- Sleight, M. A., J. R. Blake, and N. Liron. 1988. The propulsion of mucus by cilia. *Am. Rev. Respir. Dis.* 137:726–741.
- Spungin, B., and A. Silberberg. 1984. Stimulation of mucus secretion, ciliary activity, and transport in frog palate epithelium. *Am. J. Physiol.* 247:C299–C308.
- Tarasiuk, A., M. Bar-Shimon, L. Gheber, A. Korngreen, Y. Grossman, and Z. Priel. 1995. Extracellular ATP induces hyperpolarization and motility stimulation of ciliary cells. *Biophys. J.* 68:1163–1169.
- Weaver, A., and R. Hard. 1985. Newt lung ciliated cell models: effect of MgATP on beat frequency and waveform. *Cell Motil.* 5:377–392.
- Weiss, T., L. Gheber, V. Shoshan-Barmatz, and Z. Priel. 1992. Possible mechanism of ciliary stimulation by extracellular ATP: involvement of calcium-dependent potassium channels and exogenous Ca^{2+} . *J. Membr. Biol.* 127:185–193.
- Wong, L. B., I. F. Miller, and D. B. Yeates. 1991. Pathways of substance P stimulation of canine tracheal ciliary beat frequency. *J. Appl. Physiol.* 70:267–273.
- Zahm, J. M., J. Jacquot, and E. Puchelle. 1986. Ciliary beating frequency of frog palate and rat trachea explants under continuous perfusion. *Comp. Biochem. Physiol.* 85A:97–102.